Earth`s Cryosphere, 2015, vol. XIX, No. 1, pp. 88–93 **http://earthcryosphere.ru/**

EFFECT OF AIR TEMPERATURE AND SNOW DEPTH DYNAMICS ON FROST DEPTH

N.I. Osokin, A.V. Sosnovskiy

Institute of Geography, RAS,
29 Staromonetniy per., Moscow, 119017, Russia; alexandr_sosnovskiy@mail.ru

Modeling of the effect of extreme air temperature and snow depth patterns on seasonal freezing shows that seasonal variations in these parameters may cause up to 50 % difference in frost depths. The analysis is based on freezing index and snow depth ratios calculated from data of 110 weather stations for the period 1966–2010. The freezing index and snow depth dynamics over the territory of Russia are presented as maps. The dynamics of air temperatures and snow depths shows extreme behavior almost all over Russia.

Air temperature, snow depth, extreme values, frost depth

INTRODUCTION

Climate warming interferes with the thermal regime and soil freezing patterns [*Osokin et al., 2006*], including the seasonal frost depth. The variability of the soil thermal regime is commonly attributed to both air temperature and snow depth variations [*Osokin et al., 2000a*]. The former control is stronger in the East European Plain while the latter is more important in Siberia [*Sherstyukov, 2008*].

In addition to snow depth, the freezing rate depends on monthly dynamics of weather parameters, especially snow accumulation in the first half of the cold season. Small snow depth and cold air temperatures early in winter accelerate freezing [*Pavlov, 2008*], i.e., the absolute and relative (to the maximum) snow depths are critical in November and December when seasonal freezing begins. For instance, the reduced snow depth in Central Yakutia during a warm spell of 1975 through 2000 made the permafrost more stable against warming [*Skachkov, 2001*].

The effect of air temperature patterns on soil freezing is analyzed in this paper in terms of freezing index (a total of negative daily air temperatures over the cold season). This parameter is chosen because it characterizes the climate effects on freezing rates and frost depths more faithfully than mean air temperatures. For instance, data from the weather stations of Onega and Barentsburg (Spitsbergen), where the cold season has different lengths, show a freezing index difference as high as 69 % (–1130 against –1910 °C) for the period 2001–2010, while the respective difference in mean negative air temperatures is only 5 % (–7.4 against –7.8 °C) [*Osokin et al., 2012*]. Very high (or low) freezing indexes in the beginning of the cold season act upon the freezing rate and frost depth jointly with extreme snow accumulation rates (snow depths).

The objective of the study is to model the effect of extreme snow accumulation and air temperature patterns on frost depth and to analyze how this effect works in different parts of Russia.

SOIL FREEZING MODEL

The effect of extreme negative air temperatures and snow accumulation rates on soil freezing can be illustrated by a model for seasonally frozen soil. The freezing model [*Osokin et al., 2000b, 2001; Sosnovskiy, 2006*] accounts for true dynamics of air temperatures and snow depths, as well as for variations in the thermal properties of snow.

The temperature pattern of frozen soil is modeled with regard to its specific heat and thermal conductivity as a function of temperature and phase composition (water and ice content). Propagation of the frost/thaw interface (freezing front) is estimated with reference to the Stefan conditions, neglecting soil deformation and moisture flow. The boundary conditions on the soil top and base are specified, respectively, as snow-air convective heat transfer and geothermal heat flow.

The temperature (T) distribution in snow of the depth $h_s(\tau)$ at $0 < z < h_s$ is described by the Fourier equation with time-dependent thermal parameters of snow:

$$c_s \rho_s \frac{\partial T_s}{\partial \tau} = \frac{\partial T_s}{\partial z}\left(\lambda_s \frac{\partial T_s}{\partial z}\right). \quad (1)$$

The temperature distribution in frozen and unfrozen (thaw) soil is expressed using thermal conductivity equations and the dependences of the respective parameters of soil on its temperature and water content:

$$c_{ef} \rho_f \frac{\partial T_f}{\partial \tau} = \frac{\partial T_f}{\partial x}\left(\lambda_f \frac{\partial T_f}{\partial x}\right),$$

$$c_{th} \rho_{th} \frac{\partial T_{th}}{\partial \tau} = \frac{\partial T_{th}}{\partial x}\left(\lambda_{th} \frac{\partial T_{th}}{\partial x}\right). \quad (2)$$

As the boundary condition, equal temperatures and heat flows are assumed at the snow-soil interface:

$$T_s\big|_{z=0} = T_f\big|_{x=0}, \quad \lambda_s \frac{\partial T_s}{\partial z}\bigg|_{z=0} = \lambda_f \frac{\partial T_f}{\partial x}\bigg|_{x=0}. \quad (3)$$

At the frost-thaw interface, freezing is assumed to begin at T_{f0} = 272.5 K. The Stefan condition is

$$\rho_w L w_1 \frac{d\xi}{d\tau} = \lambda_f \left.\frac{\partial T_f}{\partial x}\right|_{x=\xi} - \lambda_{th} \left.\frac{\partial T_{th}}{\partial x}\right|_{x=\xi}. \qquad (4)$$

Effective bulk specific heat of frozen soil, with regard to phase transitions of unfrozen water, depends on total water content as

$$c_{e,f}(T, w_{th}) = c_f(w_{th}) + L\rho_f \frac{\partial w_w(T)}{\partial T}, \qquad (5)$$

where z and x are the spatial coordinates along snow and frost depths, respectively; T is the Kelvin temperature; τ is the time; λ is the thermal conductivity; ρ is the density; c is the specific heat; the subscripts s, f, and th refer to snow, frozen soil (frost) and unfrozen soil (thaw), respectively; c_s, c_{th} are the specific heat of snow and unfrozen soil, respectively; c_{ef} is the effective specific heat of frozen soil with regard to phase transitions of unfrozen water; L is the heat of ice melting; ξ is the interface coordinate; w_1 is the share of water freezing at the frost-thaw interface $w_1 = w_{th} - w_w$; w_{th} is the total water content of unfrozen (thaw) soil; w_w is the water content of frozen soil at the freezing front.

The variations of unfrozen water content in soil w_w were determined using curves from [*Votyakov, 1975*]; for clay silt they are approximated by the exponential function $w_w = A_1 \exp(B_1(T - 273))$, where $A_1 = 0.0834$ and $B_1 = 0.0476$.

The system of equations (1)–(5) is closed by: boundary conditions on the soil top and base; initial distribution of temperature and moisture in unfrozen soil; snow accumulation dynamics; specified variations in thermal properties of snow.

The assumed boundary conditions are as follows. Heat exchange with air on the soil (snow) surface, at $x = 0$:

$$\lambda_{f(s)} \frac{\partial T_{f(s)}}{\partial x} = Q_{th} + Q_e + Q_r - Q_{sn},$$

where Q_{th}, Q_e, Q_r, Q_{sn} are heat flows related with convective heat transfer, evaporation, effective radiation, and solar radiation, respectively.

The tabulated values of water vapor elasticity as a function of air and surface temperatures are approximated by the piecewise-linear functions $e_a = a_1 T + b_1$, where a_1, b_1 are the coefficients. Therefore, the total heat flow can be written in the convenient form as [*Kotlyakov et al., 2004*]

$$Q_\Sigma = \alpha_e \left(T_{f(s),0} - T_{ae}\right),$$

$$\alpha_e = \alpha\left(1 + 1.95 \cdot 10^{-2} a_1\right) + 0.205\left(T_a/100\right)^3,$$

$$T_{ae} = \left[\alpha\left(T_a - 1.95 \cdot 10^{-2}\left(b_1 - e_a f\right)\right) + 19.9\left(T_a/100\right)^4 + Q_{sn}\right] \Big/ \alpha_e,$$

where α_e and T_{ae} are the normalized convective heat transfer and air temperature; the heat exchange coefficients are $\alpha = v^{0.5}(7 + 7.2v^{-2})$ for soil [*Pavlov, 2008*] and $\alpha = 3.4 + 2.2v$ (where v is the wind speed and f is air humidity) for snow [*Kuzmin, 1957*]; T_a and $T_{f(s),o}$ are the Kelvin temperatures of air and surface, respectively; e_a is the water vapor elasticity in air.

The effective thermal conductivity of snow is estimated as a function of its density, using the empirical relation

$$\lambda_s = 9.165 \cdot 10^{-2} - 3.814 \cdot 10^{-4} \rho_s + 2.905 \cdot 10^{-6} \rho_s^2,$$

based on more than twenty published empirical relationships [*Osokin et al., 2001*].

The snow density (ρ, kg/m^3) is related to its depth as

$$\rho_s = 150 h_s + 120.$$

This dependence roughly corresponds to long-term means for some northern areas of West Siberia, e.g., the Berezov weather station, with the WMO code 23631 (WMO is the World Meteorological Organization).

The heat flow Q_g at the base of frozen soil is

$$\lambda_f \frac{\partial T_f}{\partial x} = Q_g,$$

where $Q_g = \lambda_f \Delta T_g$; ΔT_g is the geothermal gradient.

DATA

Modeling was applied to clay silt with the following parameters: density 1400 kg/m^3; water content 25 %; content of unfrozen water at the frost/thaw interface 11 %; thermal conductivity 1.51 and 1.33 W/(m·°C) and bulk specific heat c_f = $= 2.06 \cdot 10^6$ J/(m^3·°C) and $c_{th} = 2.78 \cdot 10^6$ J/(m^3·°C), for frozen (λ_f) and thaw (λ_{th}) soil, respectively; solar radiation was neglected.

The assumptions were: snowfall temperature equal to the air temperature; wind speed 5 m/s; air humidity 70 %; cloud cover 0.6; the lag of the snow accumulation onset behind the onset of negative daily mean temperatures (τ_{s0}) 8 days.

The extreme scenarios of air temperature and snow depth dynamics were specified (Fig. 1, *a*, *b*) at different snow accumulation rates but at the same maximum values of snow depth, amount of moisture, and thermal resistance. The scenarios differed in the depth, density, and thermal resistance of snow averaged over the cold season. The maximum snow depths were 45 and 90 cm reached at the time $\tau_{h\max}$ = 70, 140, and 210 days after the beginning of the cold season (Fig. 1, *a*).

The air temperatures were the coldest at $\tau_{T\min}$ = 70, 140, and 210 days after the beginning of the cold season (Fig. 1, *b*), the winter daily mean being about −15 °C. The soil temperature at the frost onset was assumed to be 2 °C, according to prelimi-

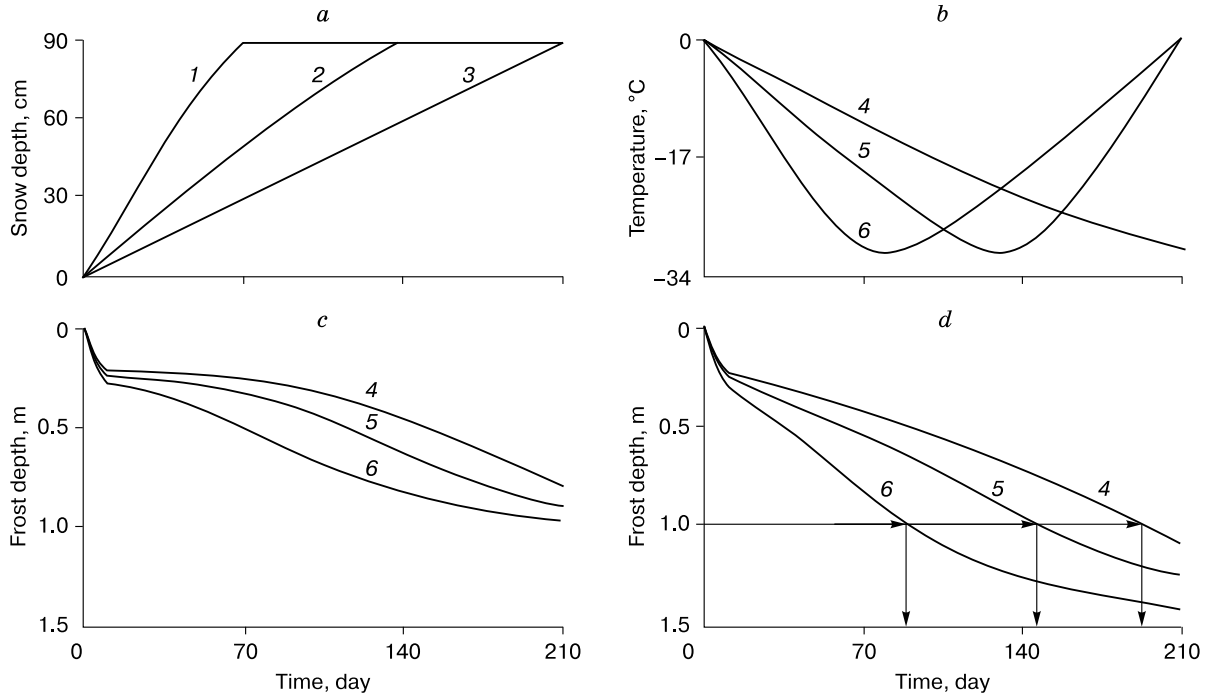

Fig. 1. Time-dependent snow depths (*a*), negative air temperatures (*b*) and frost depths (*c*, *d*) at maximum snow depth 90 cm reached 70 (*c*) and 210 (*d*) days after the cold season onset.

Curves *1*, *2*, *3* correspond to snow depths that reached the maximum at different times (t): 70 (*1*), 140 (*2*), and 210 (*3*) days after the cold season onset. Curves *4*, *5*, *6* correspond to air temperatures which were the coldest at different times (t): 210 (*4*), 140 (*5*), and 70 (*6*) days after the cold season onset. Arrows show the time when frost depth reached 1 m.

nary calculations for normal climate conditions, with the maximum snow depth in the end of the cold season and the minimum air temperature in its middle. According to calculations, a 1 °C change in soil temperature by the frost onset can cause a frost depth change of 10–15 cm.

The above system of equations for heat exchange in the system "air–snow–soil" was solved using an implicit finite-difference scheme for nonlinear heat and moisture conductivity with variable coefficients. The grid step was either fixed in space and allowed to vary in time, or fixed in time and variable in space, if necessary. In the former case, the freezing front was made to coincide with a node of a fixed spatial grid and moved to the next node at each time interval. The parameters calculated at each time step were: snow depth growth; snow density and thermal conductivity; thermal parameters of frozen and unfrozen soil; components of heat and mass transfer. If the variable time step was more than 10 % larger than the previous stepsize, further frost propagation was estimated against some intermediate position of the freezing front fixed between the spatial grid nodes.

Table 1. **Maximum frost depth at different snow depths and climate parameters**

$\tau_{T\min}$, day	$\tau_{h\max}$, day	$\xi_{\max}$, m		$\xi_{\max}/\xi_{\max}$ ($\tau_{T\min}$ = 140, $\tau_{h\max}$ = 210)	
		$h_{\max}$ = 90 cm	$h_{\max}$ = 45 cm	$h_{\max}$ = 90 cm	$h_{\max}$ = 45 cm
210	70	0.80	1.07	0.64	0.61
210	140	0.92	1.27	0.74	0.72
210	210	1.08	1.54	0.87	0.88
140	70	0.89	1.17	0.71	0.66
140	140	1.06	1.45	0.85	0.82
140	210	1.25	1.76	1.00	1.00
70	70	0.97	1.27	0.78	0.72
70	140	1.20	1.64	0.96	0.93
70	210	1.42	1.98	1.14	1.13

The maximum frost depths were calculated for two different scenarios (Fig. 1, *c*, *d*). One corresponded to the maximum snow depth 90 cm and natural snow accumulation, with the maximum snow depth in the end of the cold season ($\tau_{h\max}$ = 210 days), and the coldest air temperatures at $\tau_{T\min}$ = 140(70) days. The other scenario assumed anomalous snow accumulation, when most of frozen precipitation fell by the time $\tau_{h\max}$ = 70 days. The resulting frost depths were, respectively, $\xi_{\max}$ = 1.25(1.42) m and $\xi_{\max}$ = 0.89 (0.97) m, with their difference reaching 40 (47) %.

According to the calculation results summarized in Table 1, the frost depths 1.25 and 1.76 m correspond to the case of natural air temperature patterns ($\tau_{T\min}$ = 140 days) and maximum snow depths 90 and 45 cm, respectively, in the end of the cold season. If most of frozen precipitation falls in the first half of winter, the mean thermal resistance of snow increases and the frost depths become 29 and 34 % smaller, at the maximum snow depths $h_{\max}$ = 90 and 45 cm, respectively. The difference in the maximum frost depths between the anomalous ($\tau_{T\min}$ = 210 days, $\tau_{h\max}$ = = 70 days) and natural ($\tau_{T\min}$ = 140, $\tau_{h\max}$ = = 210 days) scenarios may reach 36 and 39 % at $h_{\max}$ = 90 and 45 cm, respectively, or even as high as 78 and 85 % at $\tau_{T\min}$ = 210, $\tau_{h\max}$ = 70 and $\tau_{T\min}$ = 70, $\tau_{h\max}$ = 210 days.

Thus, the extreme values of climate parameters and their dynamics strongly influence frost depths in seasonally frozen soil. The same must apply to seasonal thaw in zones of discontinuous and sporadic permafrost. According to Fig. 1, *d*, the freezing times of 1 m thick seasonal thaw at the maximum snow depth 90 cm, estimated for different weather parameters, at $\tau_{h\max}$ = 210 days, are approximately 95, 148 and 196 days at $\tau_{T\min}$ = 70, 140, 210 days, respectively. Therefore, variations in weather parameters control the freezing rate and time in seasonally unfrozen soil as well.

EXTREME FREEZING INDEX AND SNOW DEPTH VARIATIONS IN DIFFERENT PARTS OF RUSSIA

The conditions of the cold season in different parts of the Russian territory were analyzed using the database of the Research Institute of Hydrometeorological Information and World Data Center (RIHMI–WDC) available at http://www.meteo.ru/. For this one hundred and ten plainland weather stations were selected which provided field snow survey records, including all stations in the Arctic permafrost.

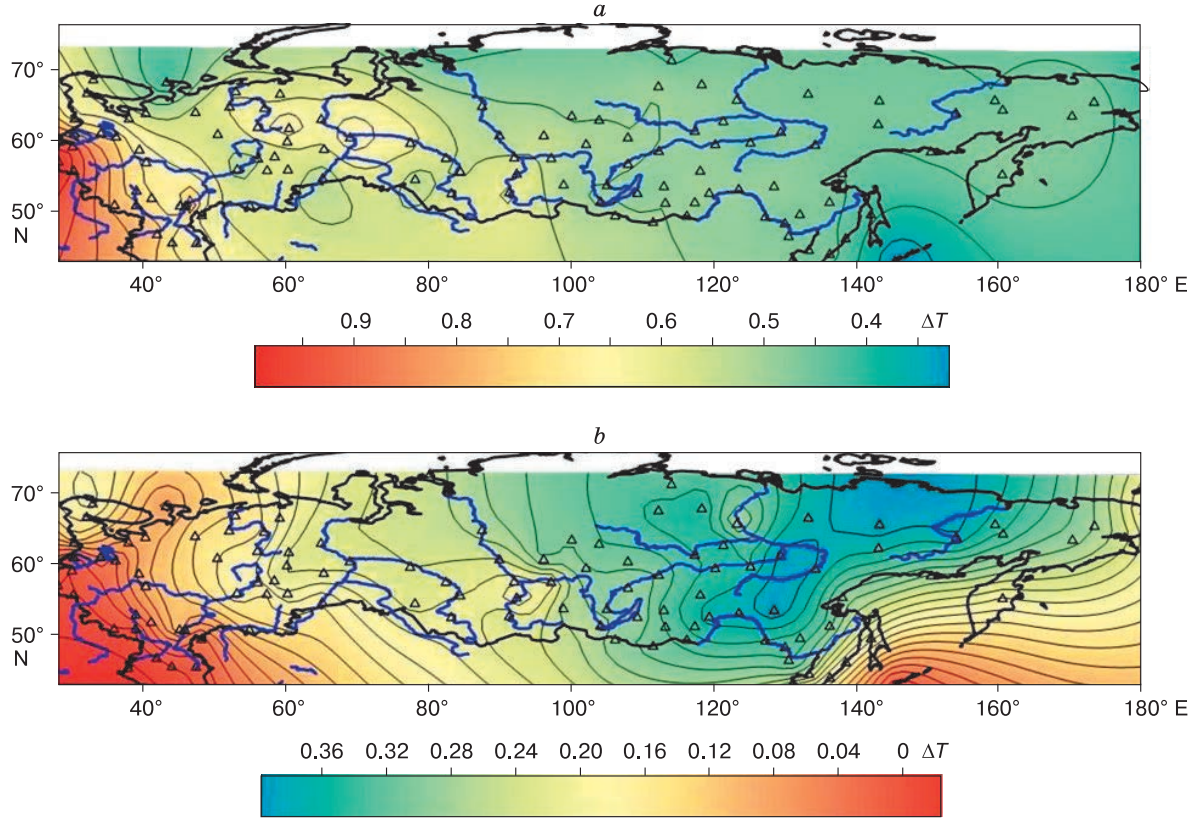

Fig. 2. Maximum (*a*) and minimum (*b*) freezing index ratios estimated as a total of negative air temperatures before January 1 divided by that over the whole cold season (ΔT) in 1966 through 2010.

Triangles are weather stations.

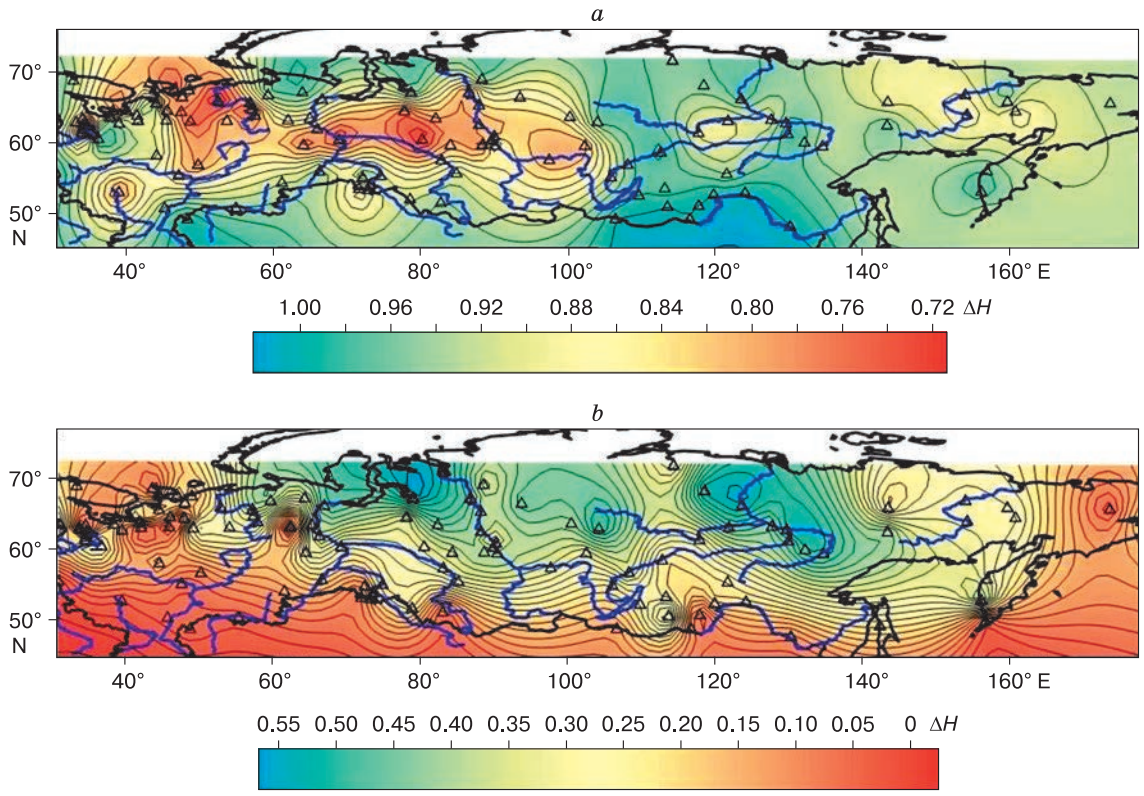

Fig. 3. Maximum (*a*) and minimum (*b*) snow depth ratios estimated as snow depths before January 1 divided by the maximum value (ΔH) in 1966 through 2010.

Triangles are weather stations.

Air temperatures were considered since 1966, the beginning of snow depth records.

The dynamics of freezing index (a total of negative air temperatures) was estimated as the ratio of its values before January 1 to those over the whole cold season (ΔT). The highest ΔT for the period of observations from 1966 through 2010 (Fig. 2, *a*) did not exceed 0.55 in Central and East Siberia (close to the long-term means 0.40–0.44), but was mostly over 0.6 in European Russia. In some years, most of negative air temperatures in southern and southwestern parts of European Russia fell within the first half of winter, and the frost depth was the largest (Fig. 1). On the other hand, air temperatures in southern Russia were sometimes negative only in the second half of winter. The lowest ΔT for 1966–2010 were in the range 0 to 0.24 in European Russia (Fig. 2, *b*) and were never below 0.32 east of the Yenisei River. Note that in no year within the 1966–2010 interval, the freezing index ratio in Siberia was less than 1/3.

The snow depth dynamics was defined by the ratio of its value before January 1, when most of freezing normally occurs, to the maximum (ΔH). The highest ΔH for the 1966–2010 period were from 0.7 to 1.0 (Fig. 3, *a*), being 0.7 in the Pechora catchment and 0.75 in the middle reaches of the Ob in some years. In southern Siberia, most of snow often fell before January 1. The lowest ΔH values for 1966–2010 (Fig. 3, *b*) were never below 0.3 over the greatest part of northern Eurasia (except western European Russia). In European Russia, snow cover formed as late as in January in some years, and snow reached only 10–15 % of its maximum depth by January 1 west of the Pechora and in southern Siberia. The small snow depths corresponded to the greatest frost depths.

Thus, the dynamics of air temperatures and snow depths shows extreme behavior almost all over Russia.

CONCLUSIONS

Modeling applied to estimate the influence of extreme air temperature and snow depth dynamics on frost depth shows that the frost depth difference may reach 50 % at different snow accumulation and air temperature patterns.

The frost depth was analyzed as controlled by the ratios of freezing index (a total of negative air temperatures) and snow depth for the period between 1966 and 2010. The freezing index ratio (ΔT) was

found as the value for the time before January 1 divided by that for the whole cold season. For snow depth it was, correspondingly, the ratio of its value before January 1 to the maximum (ΔH).

The highest ΔT for the period of observations ranged over the territory of Russia from 0.35 to 0.95 and the lowest values were within 0–0.35.

The variations of highest ΔH for the same period were 0.7 to 1.0. Most of snowfall in some areas of East Siberia occurred before January 1. The lowest ΔH were in the range 0–0.65. West of the Pechora River and in southern Siberia, only 10–15 % of the maximum snow depth formed before January 1 in some years, whereby the frost depth was the largest.

The study was carried out as part of Project 01201352476, Program 77 of the Russian Academy of Sciences.

References

Kotlyakov, V.M., Osokin, N.I., Sosnovskiy, A.V., 2004. Mathematical modeling of heat and mass exchange in snow cover during melting. Kriosfera Zemli VIII (1), 78–83.

Kuzmin, P.P., 1957. Physical Properties of Snow. Gidrometeoizdat, Leningrad, 178 pp. (in Russian)

Osokin, N.I., Samoylov, R., Sosnovskiy, A.V., Sokratov, A., 2000a. Some natural controls on soil freezing. Materialy Glaciol. Issled. 88, 41–45.

Osokin, N.I., Samoylov, R.S., Sosnovskiy, A.V., Sokratov, S.A., Zhidkov, V.A., 2000b. Model of the influence of snow cover on soil freezing. Ann. Glaciol. 31, 417–421.

Osokin, N.I., Samoylov, R., Sosnovskiy, A.V., et al., 2001. Role of snow in soil freezing. Izv. RAN, Ser. Geogr. 4, 52–57.

Osokin, N.I., Samoylov, R., Sosnovskiy, A.V., 2006. Effect of snow depth on permafrost degradation under climate warming. Izv. RAN, Ser. Geogr. 4, 40–46.

Osokin, N.I., Sosnovskiy, A.V., Nakalov, P.R., et al., 2012. Climate change and possible dynamics of permafrost in Spitsbergen. Led i Sneg, No. 2 (118), 115–120.

Pavlov, A.V., 2008. Monitoring of Permafrost. Geo Publishers, Novosibirsk, 229 pp. (in Russian)

Sherstyukov, A.B., 2008. Correlation of soil temperature with air temperature and snow cover depth in Russia. Kriosfera Zemli XII (1), 79–87.

Skachkov, Yu.B., 2001. Thermal Stability of the Upper Permafrost in Central Yakutia in the Course of Current Warming. Author's Abstract, Candidate Thesis, Yakutsk, 25 pp. (in Russian)

Sosnovskiy, A.V., 2006. Mathematical modelling of the influence of snow cover thickness on degradation of permafrost at climate warming. Kriosfera Zemli X (3), 83–88.

Votyakov, I.N., 1975. Mechanical Properties of Frozen and Unfrozen Soils in Yakutia. Nauka, Novosibirsk, 176 pp. (in Russian)

URL: http://www.meteo.ru (last access 21.03.2013). RIHMI–WDC.

Received October 31, 2013